

A Quantum Switch for Superconducting Resonators in Circuit QED

Matteo Mariantoni^{*,1,†} Frank Deppe^{*,1} A. Marx,¹ R. Gross,¹ F. K. Wilhelm,² and E. Solano^{3,4}

¹Walther-Meißner-Institut, Bayerische Akademie der Wissenschaften,
Walther-Meißner-Strasse 8, D-85748 Garching, Germany

²IQC and Department of Physics and Astronomy, University of Waterloo,
200 University Avenue West, Waterloo, Ontario, N2L 3G1, Canada

³Physics Department, CeNS and ASC, Ludwig-Maximilians-Universität, Theresienstrasse 37, D-80333 Munich, Germany

⁴Sección Física, Departamento de Ciencias, Pontificia Universidad Católica del Perú, Apartado 1761, Lima, Peru

(Dated: May 27, 2019)

We demonstrate that a superconducting qubit can function as a quantum switch between two independent on-chip microwave resonators, which are simultaneously coupled to it. In this three-circuit network, the qubit mediates a *geometric second-order circuit* interaction between the otherwise decoupled resonators. In the dispersive regime, it also gives rise to a *dynamic second-order perturbation* interaction. The geometric and dynamic coupling strengths can be tuned to be equal, thus permitting to switch on and off the interaction between the two resonators via a qubit population inversion. We also discuss the robustness of this quantum switch to decoherence mechanisms and give a few examples of its use for the generation of multipartite entanglement in circuit QED.

PACS numbers: 03.67.Lx,42.50.Pq,84.30.Bv,32.60.+i

In the past few years, we have witnessed a tremendous experimental progress in the flourishing realm of circuit QED [1, 2]. There, different types of superconducting qubits have been strongly coupled to on-chip microwave resonators, which act as quantized cavities. Recently, a quantum state has been stored and coherently transferred between two superconducting phase qubits via a microwave resonator [3] and two transmon qubits have been successfully coupled utilizing an on-chip cavity as a quantum bus [4]. Furthermore, microwave single photons have been generated by spontaneous emission [5] and lasing effects demonstrated exploiting three charge states of a single Cooper-pair box [6]. These formidable advances show how circuit QED systems are rapidly reaching a level of complexity comparable to the already well-established quantum optical cavity QED [7, 8, 9].

Amongst the aims common to these experiments is the possibility to perform quantum information processing [10], where certain tasks can be achieved following the lines of recent proposals [11, 12]. The latter considers a two-dimensional array of on-chip resonators coupled to qubits. In this or any other multi-cavity setup, it is highly desirable to switch on and off an interaction between two resonators or to compensate their spurious crosstalk.

In this manuscript, we theoretically study a three-circuit network where a superconducting charge or flux qubit [13, 14] interacts with two on-chip microwave cavities. In the absence of the qubit, the resonators are assumed to have negligible or small direct crosstalk. This scenario seems to be similar to that of quantum optics where an atom can interact with two orthogonal cavity modes [15], but there are some crucial differences.

The system dynamics cannot be described within a simple two-mode Jaynes-Cummings (JC) model. In fact, the nature of the three-circuit system considered here imposes to account for a *geometric second-order circuit* interaction between the two resonators, giving rise to beam-splitter coupling terms. This interaction is mediated by the circuit part of the qubit, but does not depend on the qubit state. It is noteworthy to mention that this coupling does not exist in the two-mode JC model, showing a departure from the neat analogy between cavity and circuit QED valid in the case of a single cavity [16, 17]. In the dispersive regime, when the transition frequency of the qubit is largely detuned from that of the cavities, the usual beam-splitter interaction terms between the two resonators also appear. They result from a *dynamic second-order perturbation* interaction and depend on the state of the qubit. The sign of the interaction can be changed by an inversion of the qubit population. Notably, for a suitable set of parameters, the geometric and dynamic second-order coupling coefficients can be made exactly equal by choosing a proper qubit-resonator detuning. In this case, the interaction between the two cavities can be switched on and off, thereby enabling the implementation of a discrete quantum switch.

The system to be studied is sketched in Figs. 1 (a) and (b), where the microwave resonators have been represented by symbolic mirrors. A and B represent the two cavities and Q a superconducting qubit (hereafter also labeled as 1, 2, and 3, respectively), making altogether a three-circuit network. The coupling channels between the three circuits are assumed to be capacitive and/or inductive. We also hypothesize the direct interaction between A and B to be weak and that between A or B and Q to be strong. In other words, the first-order capacitance and inductance matrices are

*Authors with equal contribution to this work.

$\mathbf{C} = C_{kl}$ and $\mathbf{M} = M_{kl}$, with $k, l \in \{1, 2, 3\}$, where $C_{kl} = C_{lk}$ and $M_{kl} = M_{lk}$ because of symmetry reasons. In addition, we assume $C_{12} \equiv c \ll C_{kl \neq 12, 21}$ and $M_{12} \equiv m \ll M_{kl \neq 12, 21}$. The elements c and m represent a small direct crosstalk between A and B, which can have a spurious or engineered origin. If the resonators are single-mode cavities, the total Hamiltonian of the system is given by [14, 18]

$$\hat{H}_T = \frac{1}{2} \vec{V}^T \mathbf{C}^{(n)} \vec{V} + \frac{1}{2} \vec{I}^T \mathbf{M}^{(n)} \vec{I} + \frac{1}{2} G(E_J, E_c) \hat{\sigma}_x, \quad (1)$$

where $\mathbf{C}^{(n)}$ and $\mathbf{M}^{(n)}$ are the renormalized capacitance and inductance matrices up to the n -th order, with $\mathbf{C}^{(1)} \equiv \mathbf{C}$ and $\mathbf{M}^{(1)} \equiv \mathbf{M}$. Also, $\vec{V} \equiv [\hat{V}_1, \hat{V}_2, \hat{V}_3]^T$ and $\vec{I} \equiv [\hat{I}_1, \hat{I}_2, \hat{I}_3]^T$, G , in general, is a function of the coupling energy E_J and/or charging energy E_c of the Josephson tunnel junctions in the qubit (for instance, $G = E_J$ for a charge qubit and $G \propto \sqrt{E_J E_c} \exp(-\sqrt{E_J/E_c})$ for a flux qubit), $\hat{V}_1 \equiv v_{\text{DC}} + v_{a0}(\hat{a}^\dagger + \hat{a})$, $\hat{V}_2 \equiv v_{b0}(\hat{b}^\dagger + \hat{b})$, $\hat{V}_3 \equiv v_q \hat{\sigma}_z$, $\hat{I}_1 \equiv i_{\text{DC}} + i_{a0} j(\hat{a}^\dagger - \hat{a})$, $\hat{I}_2 \equiv i_{b0} j(\hat{b}^\dagger - \hat{b})$, and $\hat{I}_3 \equiv i_q \hat{\sigma}_z$. In these expressions, $\hat{\sigma}_x$ and $\hat{\sigma}_z$ are the usual Pauli matrices for a spin-1/2 system in the bare basis ($|-\rangle$ and $|+\rangle$), \hat{a}^\dagger , \hat{b}^\dagger , \hat{a} , and \hat{b} are bosonic creation and annihilation operators for the fields of cavities A and B, respectively, and $j \equiv \sqrt{-1}$. The DC voltage v_{DC} and current i_{DC} account for the quasi-static polarization of the qubit and can be applied through any suitable bias circuit. For definiteness, we have chosen cavity A to perform this function [1]. The vacuum fluctuations of the voltage and current of each resonator are given by $v_{a0} \equiv \sqrt{\hbar \omega_a / 2 C_{11}}$, $v_{b0} \equiv \sqrt{\hbar \omega_b / 2 C_{22}}$, $i_{a0} \equiv \sqrt{\hbar \omega_a / 2 L_{11}}$, and $i_{b0} \equiv \sqrt{\hbar \omega_b / 2 L_{22}}$, respectively, with ω_a and ω_b the transition angular frequencies of the two cavities. Finally, v_q and i_q represent the voltage of the superconducting island(s) and the current through the loop of the qubit circuit. Depending on the specific qubit implementation, either v_q or i_q dominates, thus defining the charge and flux regimes.

The matrices $\mathbf{C}^{(n)}$ and $\mathbf{M}^{(n)}$ account for corrections up to the n -th order interaction process between the elements of the network. In fact, in order to write the exact Hamiltonian of the circuit, all possible electromagnetic paths connecting its nodes must be considered. A consequence of this approach to circuit theory is that not only the direct coupling between resonators A and B ($\hat{H}_{12}^{(1)} = \hat{V}_1 c \hat{V}_2 + \hat{I}_1 m \hat{I}_2$, here assumed to be small), but also an indirect coupling mediated by the circuit Q have to be included in the Hamiltonian. The dominating term for the A-Q-B (1-3-2) excitation pathway can be derived from its second order electromagnetic energy, which gives

$$\hat{H}_{12}^{(2)} = \hat{H}_{12}^{(1)} + \hat{V}_1 C_{13} \frac{1}{C_{33}} C_{32} \hat{V}_2 + \hat{I}_1 M_{13} \frac{1}{M_{33}} M_{32} \hat{I}_2. \quad (2)$$

Note that the inverse path (2-3-1) is already included in Eq. (2). In our work, $0 \lesssim c \lesssim C_{13} C_{31} / C_{33}$ and $0 \lesssim m \lesssim M_{13} M_{31} / M_{33}$. When $c, m \sim 0$, the direct coupling between A and B is negligible, i.e., the contribution of $\hat{H}_{12}^{(1)}$ can be omitted. On the other hand, when $c > 0$ and/or $m > 0$, both first-order and second-order circuit theory contributions are relevant. In this case, c and m can represent a spurious or an engineered crosstalk. The latter can be deliberately exploited to increase the strength of the geometric second order couplings. However, c and m should be small enough to leave the mode structure and quality factors of A and B unaffected.

From the knowledge of $\hat{H}_{12}^{(2)}$, the capacitance matrix up to second order is readily obtained

$$\mathbf{C}^{(2)} = \begin{bmatrix} C_{11} & c + \frac{C_{13} C_{32}}{C_{33}} & C_{13} \\ c + \frac{C_{23} C_{31}}{C_{33}} & C_{22} & C_{23} \\ C_{31} & C_{32} & C_{33} \end{bmatrix}. \quad (3)$$

In analogy, the corrected inductance matrix $\mathbf{M}^{(2)}$ is found substituting C_{kl} with M_{kl} and c with m in Eq. (3).

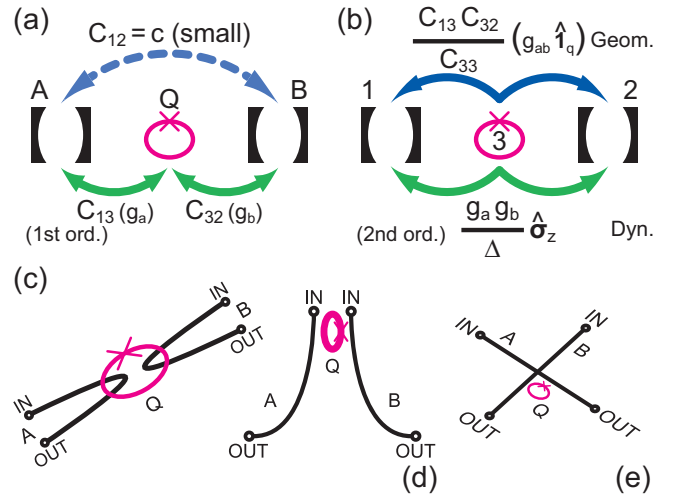


FIG. 1: (color online). Sketch of the system under analysis. (a) Schematic representation of the first order Hamiltonian $\hat{H}^{(1)}$. Two cavities A and B interact with a generic superconducting qubit Q. A and B can have a weak coupling c [blue (grey) broken arrow]. The two green (light grey) arrows represent a two-mode JC dynamics with coupling coefficients g_a and g_b , respectively. (b) The effective second order Hamiltonian \hat{H}_{eff} of Eq. (6). The blue (dark grey) arrows show the *geometric* coupling channel mediated by a virtual excitation of Q, whereas the green (light grey) arrows the *dynamic* channel. (c) Setup topology 1. A flux qubit (Q) sits at the current antinode of two $\lambda/2$ resonators (A and B; first mode). Only the inner conductor is shown. At the “IN” and “OUT” ports there will be coupling capacitors. (d) Setup topology 2. A charge qubit sits at the voltage antinode of two cavities (e.g., first mode). (e) Setup topology 3. A charge or flux qubit sits at the voltage (e.g., second mode) or current (e.g., first mode) antinode of two crossed resonators [12].

We are now able to give the total Hamiltonian of the three-circuit quantum network of Figs. 1 (a) and (b). In order to avoid cumbersome calculations, we restrict ourselves to purely capacitive interactions up to second order corrections. In this particular case, we can consider the vacuum fluctuations v_{a0} and v_{b0} to have maximum values v_{a0}^{\max} and v_{b0}^{\max} , respectively, at the qubit position (a voltage antinode). As a consequence, we can impose $i_{a0} = i_{b0} = 0$ and retain only the DC inductive couplings. Also, $\mathbf{C}^{(n)}$ of Eq. (1) is substituted by $\mathbf{C}^{(2)}$ of Eq. (3). We straightforwardly obtain

$$\begin{aligned} \widehat{H} = & \frac{1}{2}\hbar\epsilon\hat{\sigma}_z + \frac{1}{2}\hbar\delta\hat{\sigma}_x + \hbar\omega_a\hat{a}^\dagger\hat{a} + \hbar\omega_b\hat{b}^\dagger\hat{b} \\ & + v_{\text{DC}}K_a(\hat{a}^\dagger + \hat{a}) + v_{\text{DC}}K_b(\hat{b}^\dagger + \hat{b}) \\ & + \hbar g_a\hat{\sigma}_z(\hat{a}^\dagger + \hat{a}) + \hbar g_b\hat{\sigma}_z(\hat{b}^\dagger + \hat{b}) \\ & + \hbar g_{ab}(\hat{a}^\dagger + \hat{a})(\hat{b}^\dagger + \hat{b}) \quad , \end{aligned} \quad (4)$$

where all global energy offsets have been neglected and we have included both first-order and second-order circuit theory contributions. The coefficients ϵ , δ , ω_a , ω_b , K_a , and K_b are defined in Ref. [20] and $g_a \equiv v_q v_{a0} C_{13}/\hbar$, $g_b \equiv v_q v_{b0} C_{23}/\hbar$, and the second order coupling $g_{ab} \equiv v_{a0} v_{b0} (c + C_{13} C_{32}/C_{33})/\hbar$. In general, g_a and g_b are different and, if needed, they can be engineered to be practically equal (see, e.g., Ref. [4]). Moving to the qubit energy basis (with redefined Pauli matrices $\hat{\sigma}_x$, $\hat{\sigma}_y$, and $\hat{\sigma}_z$) allows us to write the qubit Hamiltonian as $\widehat{H}_q = \hbar\Omega_q\hat{\sigma}_z/2$, where $\Omega_q = \sqrt{\epsilon^2 + \delta^2}$ is a function of both v_{DC} and i_{DC} . In addition, the usual mixing angle $\theta = \arctan(\delta/\epsilon)$ can be defined. Expressing the transformed Hamiltonian in an interaction picture with respect to the qubit and both resonators, assuming $\omega_a = \omega_b \equiv \omega$, and performing a rotating wave approximation (RWA), yields

$$\begin{aligned} \widehat{H} = & \hbar \sin\theta \left[\hat{\sigma}^- (g_a \hat{a}^\dagger + g_b \hat{b}^\dagger) e^{-j\Delta t} + \hat{\sigma}^+ (g_a \hat{a} + g_b \hat{b}) e^{j\Delta t} \right] \\ & + \hbar g_{ab} (\hat{a}^\dagger \hat{b} + \hat{a} \hat{b}^\dagger) \quad , \end{aligned} \quad (5)$$

where $\Delta \equiv \Omega_q - \omega$ and $\hat{\sigma}^-$ and $\hat{\sigma}^+$ are the usual qubit lowering and raising operators between its energy ground and excited states, $|g\rangle$ and $|e\rangle$, respectively. The first two terms of Eq. (5) represent a standard two-mode JC dynamics [15] and the last one a beam-splitter type of interaction, which is not present in the quantum optical version. The coupling coefficient g_{ab} is typically much smaller than g_a and g_b (see below). However, in the dispersive regime ($|\Delta| \gg \{g_a, g_b, g_{ab}\}$), g_{ab} becomes comparable to all other dispersive coupling strengths. To gain further insight into this matter, we can define two superoperators $\widehat{\Xi}^\dagger \equiv \hat{\sigma}^+ (g_a \hat{a} + g_b \hat{b})$ and $\widehat{\Xi} \equiv \hat{\sigma}^- (g_a \hat{a}^\dagger + g_b \hat{b}^\dagger)$. It can be shown that the

Dyson series for the evolution operator associated with the time-dependent Hamiltonian of Eq. (5) can be rewritten in an exponential form $\widehat{U} = \exp(-j\widehat{H}_{\text{eff}}t/\hbar)$, where $\widehat{H}_{\text{eff}} = \hbar [\widehat{\Xi}^\dagger, \widehat{\Xi}] / \Delta + \hbar g_{ab} (\hat{a}^\dagger \hat{b} + \hat{a} \hat{b}^\dagger)$ [19]. Thus

$$\begin{aligned} \widehat{H}_{\text{eff}} = & \hbar \frac{(g_a \sin\theta)^2}{\Delta} \hat{\sigma}_z \left(\hat{a}^\dagger \hat{a} + \frac{1}{2} \right) \\ & + \hbar \frac{(g_b \sin\theta)^2}{\Delta} \hat{\sigma}_z \left(\hat{b}^\dagger \hat{b} + \frac{1}{2} \right) \\ & + \hbar \left(\frac{g_a g_b \sin^2\theta}{\Delta} \hat{\sigma}_z + g_{ab} \right) (\hat{a}^\dagger \hat{b} + \hat{a} \hat{b}^\dagger) \quad , \end{aligned} \quad (6)$$

which constitutes the central result of this work. In this Hamiltonian, the first two terms represent dynamic (AC-Stark or -Zeeman) shifts of the transition angular frequency of resonators A and B, respectively. If $g_a \sim g_b$ and we only use eigenstates of $\hat{\sigma}_z$, the first two terms of Eq. (6) equally renormalize ω_a and ω_b , respectively. When $g_a \neq g_b$, it is still possible to retune *in situ* those shifts by means of a further (coherent state induced) AC-Stark or -Zeeman shift [4]. The last term of Eq. (6) is the key ingredient for the implementation of a quantum switch. In fact, it clearly represents an interaction between A and B characterized by an effective coupling coefficient $g_{\text{sw}}^{(|g\rangle, |e\rangle)} \equiv g_a g_b \sin^2\theta / \Delta \mp g_{ab}$ for $|g\rangle$ and $|e\rangle$, respectively. The switching of such an interaction will trigger, or prevent, the exchange of quantum information between A and B. The first part of this interaction is a dynamic coupling, which depends on the state of the qubit, whereas the second is a purely geometric coupling, which is constant and qubit-state independent. The *switch setting condition* $g_a g_b \sin^2\theta / |\Delta| = g_{ab}$ can be easily fulfilled by adjusting the qubit operation point. This means changing $\sin\theta$ and, consequently, also Δ .

A possible switching protocol follows. (i) - The quasi-static bias of the qubit is chosen such that the switch setting condition is fulfilled. This will typically happen away from the qubit degeneracy point. (ii) - For the switch operation to be practical, we choose $\Delta > 0$. This guarantees that the sign in front of the $\hat{\sigma}_z$ operator of Eq. (6) remains positive and, as a consequence, the switch is off ($g_{\text{sw}}^{(|g\rangle)} = 0$) in state $|g\rangle$ and on ($g_{\text{sw}}^{(|e\rangle)} = 2g_{ab}$) in state $|e\rangle$. (iii) - There are now two possible pulse schemes, (a) and (b), for the operation of the quantum switch with the qubit in the energy ground state. (a) - The qubit is maintained at the bias point preset in i) and a Rabi π -pulse is applied in order to perform a population inversion from $|g\rangle$ to $|e\rangle$. The sign given by the $\hat{\sigma}_z$ operator for a different qubit state is exploited to switch on and off the interaction between A and B. In this case, the switching time is $t_{\text{sw}} = 1/g_{\text{sw}}^{(|e\rangle)}$, which has to be shorter than both resonators' decay times ($1/\kappa_a$ and $1/\kappa_b$, respectively) and the qubit energy relaxation time $1/\gamma_q^{\text{eff}}$. The latter is further enhanced compared to its intrinsic

value because of the dispersive condition [17] and, away from degeneracy, of a reduced $\sin\theta$. Here, dephasing might become worse. However, since only virtual excitations between each cavity and the qubit are allowed, dephasing mechanisms are not the limiting factor. This is evident from \hat{H}_{eff} of Eq. (6), where only $\hat{\sigma}_z$ terms are present and, thus, only the qubit populations are effectively utilized during the switching protocol. In other words, the qubit behaves as a dephasing-free quantum bus in a dual setup compared to that of Ref. [4]. (b) - An adiabatic pulse is applied to opportunely shift the qubit away from the switch setting condition defined in *i*) to a new point $|\tilde{g}\rangle$. Consequently, the dynamic and geometric couplings are not balanced anymore and the switch is set from off to on with a new coupling $\tilde{g}_{\text{sw}} \lesssim 2g_{\text{ab}}$. The rise time of the shift pulse has to fulfill the condition $1/\delta, 1/\omega < \tau_{\text{rise}} < 1/2g_{\text{ab}}$ [2]. In this case, the switch is also robust to energy relaxation mechanisms.

We now provide a few pedagogical examples to clarify the physics of our quantum switch. First, we assume that a Fock state $|1\rangle_{\text{A}}$ is prepared in cavity A (e.g., by means of another qubit coupled to it), while cavity B remains in the vacuum state $|0\rangle_{\text{B}}$. Then, the above protocol allows the generation of coherent linear superpositions $\cos(2g_{\text{ab}}t)|1\rangle_{\text{A}}|0\rangle_{\text{B}} + e^{j\phi}\sin(2g_{\text{ab}}t)|0\rangle_{\text{A}}|1\rangle_{\text{B}}$ (ϕ is a generic phase) as a function of the switching operation time t . Depending on the chosen t , this can be used as a mechanism for transferring the single photon from A to B or for generating controlled entanglement between the two cavities. Second, when the qubit is prepared in a linear superposition $(|g\rangle + |e\rangle)/\sqrt{2}$, and after a pulse corresponding to $t = \pi/4g_{\text{ab}}$, the dynamics yields the state $(|g\rangle|1\rangle_{\text{A}}|0\rangle_{\text{B}} + |e\rangle|0\rangle_{\text{A}}|1\rangle_{\text{B}})/\sqrt{2}$. This represents a tripartite entangled state of the GHZ class [21] and contains maximal entanglement for the three-qubit case. Finally, if the initial state in cavity A is a coherent state $|\alpha\rangle_{\text{A}}$ and cavity B remains in $|0\rangle_{\text{B}}$, we will be able to generate nonlocal Schrödinger cat states [8, 22].

We notice that there can be other tuning possibilities to reach the switch setting condition *in situ*, besides changing $\sin\theta$. For instance, G can effectively be modified by a suitable DC biasing [1, 23] and/or dynamic shifts induced by off-resonant coherent states [4]. Based on our previous arguments dephasing induced by photon shot noise is also not an issue. In addition, the role played by c and m becomes now evident. If they represent a spurious coupling between A and B (e.g., in the cavity grid architecture of Ref. [12]), our switch can be used to correct them and erase the harmful crosstalk. For instance, a quantum switch can be positioned at the edge of each cavity in the grid. In other cases, small c and m can be suitably engineered to increase the total g_{ab} in order to improve the tunability of the system.

Extrapolating the capacitance and inductance matrices from Refs. [2, 4, 23], we find that coupling strengths $g_{\text{ab}} \in (1, 5)$ MHz can be easily achieved for de-

tunings $\Delta \in (0.5, 5)$ GHz and a $\sin\theta \in (0.8, 0.95)$. The constants g_{ab} are larger than the typical values for cavities' and qubit's decay rates $\kappa_{\text{a}}, \kappa_{\text{b}}, \gamma_{\text{q}}^{\text{eff}} \lesssim 1$ MHz. We refer to Figs. 1 (c), (d), and (e) for three possible topological structures to implement our switch.

In conclusion, we have derived a Hamiltonian describing the interaction of a superconducting qubit with two resonators which have negligible or small direct coupling. We have studied the topology of this network using a higher-order circuit theory approach and shown that, when the cavities are largely detuned from the qubit, two distinguished second order processes can compete: A dynamic and a geometric interaction. This allows the implementation of a quantum switch between the two resonators with a reduced sensitivity to decoherence.

This project is partially funded by the German Science Foundation through SFB 631, EU EuroSQIP and NSERC projects, and the German Excellence Initiative via NIM. We thank E. P. Menzel for fruitful discussions.

[†] Electronic address: Matteo.Mariantoni@wmi.badw.de

- [1] A. Wallraff *et al.*, Nature (London) **431**, 162 (2004).
- [2] J. Johansson *et al.*, Phys. Rev. Lett. **96**, 127006 (2006).
- [3] M. A. Sillanpää, J. I. Park, and R. W. Simmonds, Nature (London) **449**, 438 (2007).
- [4] J. Majer *et al.*, Nature (London) **449**, 443 (2007).
- [5] A. A. Houck *et al.*, Nature (London) **449**, 328 (2007).
- [6] O. Astafiev *et al.*, Nature (London) **449**, 588 (2007).
- [7] H. Mabuchi and A. C. Doherty, Science **298**, 1372 (2002).
- [8] S. Haroche and J.-M. Raimond, *Exploring the Quantum*, (Oxford University Press Inc., New York, 2006).
- [9] H. Walther, B. T. H. Varcoe, B. G. Englert, and T. Becker, Rep. Prog. Phys. **69**, 1325 (2006).
- [10] M. A. Nielsen and I. L. Chuang, *Quantum Computation and Quantum Information*, (Cambridge University Press, Cambridge, 2000).
- [11] A. Blais *et al.*, Phys. Rev. A **75**, 032329 (2007).
- [12] F. Helmer *et al.*, eprint arXiv:0706.3625 (unpublished).
- [13] Yu. Makhlin, G. Schön, and A. Shnirman, Rev. Mod. Phys. **73**, 357 (2001).
- [14] M. H. Devoret, A. Wallraff, and J. M. Martinis, eprint arXiv:cond-mat/0411174 (unpublished).
- [15] A. Rauschenbeutel *et al.*, Phys. Rev. A **64**, 050301 (2001).
- [16] J. Q. You and F. Nori, Phys. Rev. B **68**, 064509 (2003).
- [17] A. Blais *et al.*, Phys. Rev. A **69**, 062320 (2004).
- [18] L. O. Chua, C. A. Desoer, and E. S. Kuh, *Linear and Nonlinear Circuits*, (McGraw-Hill C., New York, 1987).
- [19] M. Mariantoni *et al.*, in preparation.
- [20] The coefficients are $\epsilon \equiv 2v_{\text{q}}v_{\text{DC}}C_{13}/\hbar + 2i_{\text{q}}i_{\text{DC}}M_{13}/\hbar$, $\delta \equiv E_{\text{J}}/\hbar$, $\omega_{\text{a}} \equiv 1/\sqrt{C_{11}M_{11}}$, $\omega_{\text{b}} \equiv 1/\sqrt{C_{22}M_{22}}$, $K_{\text{a}} \equiv v_{\text{a}0}(C_{11} + C_{13})/2$, and $K_{\text{b}} \equiv v_{\text{b}0}C_{13}C_{32}/C_{33}$.
- [21] W. Dür, G. Vidal, and J. I. Cirac, Phys. Rev. A **62**, 062314 (2000).
- [22] L. Davidovich *et al.*, Phys. Rev. Lett. **71**, 2360 (1993).
- [23] R. H. Koch *et al.*, Phys. Rev. Lett. **96**, 127001 (2006).